

Power Quality and Unbalanced Conditions Assessment Based on Digital Fault Recorders(DFRs)

Huiying Huang

Thesis submitted to the Faculty of the
Virginia Polytechnic Institute and State University
in partial fulfillment of the requirements for the degree of

Master of Science
in
Electric Engineering

Jaime De La Ree Lopez, Chair
Virgilio A. Centeno
Vasileios. Kekatos

December 7 , 2017
Blacksburg, Virginia

Keywords: Power Quality, Data Visualization, Unbalanced Conditions, Harmonics
Copyright 2017, Huiying Huang

Power Quality and Unbalanced Conditions Assessment Based on Digital Fault Recorders(DFRs)

Huiying Huang

ABSTRACT

With the rapid development of power systems, more and more smart devices are installed in power industries, and each of them is gathering tons of information every day. Due to the data explosion and the difficulty of processing these data, data visualization, a big data technology, has become a trend. With the help of information technology, the visualization of real-time data has been achieved in power industries and there are multiple successful examples such as one-line diagram, load flow dashboard and equipment dashboard. In fault analysis group, digital fault recorders are essential to record and report an event. They are triggered when a fault occurs and corresponding report is generated instantly. However, people seldom utilize the historical data from DFRs to analyze the power quality issues. Therefore, this thesis presents the development of a power quality dashboard by using the collected data from DFRs. Three related power quality analyses have been accomplished in this paper: voltage and current variation, harmonics and unbalance components. Recursive algorithm is applied to compute the phasors and errors; Discrete Fourier Transform is utilized to extract harmonics from the samples; and the symmetric components are calculated by "A"-matrix transformation. The start page for the dashboard is a google map with all the DFR markers, and after double-clicking the marker, the report page will be opened. With the reports, engineers can not only monitor the event but also analyze out the possible causes and characteristics for a fault. For those renewable energy substation, the harmonic contents can be supervised so that the damages and losses can be significantly reduced by identifying the high harmonics. Ultimately, the goal of the dashboard is to achieve warning status and

harmonic gradient mapping in the future.

Power Quality and Unbalanced Conditions Assessment Based on Digital Fault Recorders(DFRs)

Huiying Huang

GENERAL AUDIENCE ABSTRACT

Power quality becomes a hot topic as electricity is more and more important in our daily life. In power industries, many devices such as PMU, SCADA, DFR are installed to monitor the power systems. These devices can not only provide real-time status, but also records that can be utilized for advanced research. To manage the massive quantity data from the records, data visualization has been widely applied in utilities. Because of the success of those visualization tools such as one-line diagrams, equipment dashboard, DFR dashboard, a new power quality dashboard is accomplished in this thesis. It provides the sample values and estimated values for voltage and current, the Index of Variance, harmonic contents and symmetrical components. Engineers can monitor power quality issues from the dashboard. Meanwhile, they can analyze possible causes and characteristics of a fault from unbalanced conditions.

ACKNOWLEDGEMENT

I would first like to express my appreciation to my advisor Dr. Jaime De La Ree Lopez at Virginia Tech. The door to his office was always open whenever I ran into a trouble spot or had a question about my research. He consistently allowed this paper to be my own work, but steered me in the right direction whenever he thought I needed it. Besides the precious ideas that he provided to me, he also becomes my friend in my life. I would also like to thank to my committee members Dr. Virgilio. A. Centeno and Dr. Vassilis Kekatos for their support of my research and study.

I would like to thank to my lab-mates in power lab. They always provide me suggestions, answer my questions whenever I ask them. To Xiawen Li and Xiaolan Zou, I want to thank you to be my office-mates. You never hesitate to help me whenever I get into trouble with my study, research, or even life.

In the end, I must express my very profound gratitude to my father Fu Huang and my mother Jian Gao for providing me with unfailing support and continuous encouragement throughout my years of study and the process of researching and writing this thesis. This accomplishment would not have been possible without them.

Contents

- List of Figures** **viii**

- List of Tables** **x**

- 1 Introduction** **1**
 - 1.1 Introduction 1
 - 1.2 Outline of The Thesis 2

- 2 Background and Related Acknowledgment** **3**
 - 2.1 The Importance of Power Quality 3
 - 2.1.1 Definition of Power Quality 3
 - 2.1.2 The Importance of Power Quality 5
 - 2.1.3 Power Quality Evaluation Procedure 5
 - 2.2 Digital Fault Recorders (DFRs) 7
 - 2.2.1 Definition 7
 - 2.2.2 COMTRADE Standard 8
 - 2.3 Data Visualization In Power Systems 9
 - 2.3.1 Introduction of Big Data 9
 - 2.3.2 Data Visualization in Power systems 10

- 3 The Design of Power Quality Dashboard** **13**
 - 3.1 Motivation of The Project 13
 - 3.2 Related Analyses for Power Quality Problems 16

3.2.1	Phasor Estimation	16
3.2.2	Harmonic Contents	22
3.2.3	Imbalance Components	24
3.3	Dashboard Design	27
4	Results and Case Study	30
4.1	The Details of Power Quality Dashboard	30
4.2	Case Study	33
4.2.1	Normal Result Without Power Quality Issue	34
4.2.2	Results For Harmonic Contents	35
4.2.3	Results For Unbalance Components	40
4.2.4	Results With Fault And Their Analysis With Unbalanced Conditions	42
5	Conclusion and Future Work	46
5.1	Summary	46
5.2	Future Work	48
	Reference	51

List of Figures

- 2.1 Steps of a power quality evaluation. 6
- 2.2 Procedures to realize data visualization. 10
- 2.3 An example of data visualization - DFR dashboard in Dominion Energy. . . 11

- 3.1 One-line diagrams are widely used in power industries. 14
- 3.2 Reactor banks dashboard in Dominion Energy. 15
- 3.3 Sinusoidal waveform and its phasor representation. 17
- 3.4 Spectrum of a band-limited signal with spectral overlap. 23
- 3.5 Procedure of data server-client application implementation. 29

- 4.1 The start page of power quality dashboard. 30
- 4.2 DFR Information will be displayed when the marker is clicked. 31
- 4.3 The marker will link to a report page after double clicking it. 31
- 4.4 Current harmonic contents report page. 32
- 4.5 Current unbalance report page. 33
- 4.6 Normal report of phasor estimation without power quality issue. 34
- 4.7 Normal report of current unbalance components without power quality issue. 35
- 4.8 Reports of phasor estimation for a substation connected to a solar generator. 36
- 4.9 Harmonic contents against time for substation connected to a solar generator. 37
- 4.10 Second reports of phasor estimation for a substation connected to a solar generator. 38
- 4.11 Harmonic contents for the second result. 39
- 4.12 Phasor estimation for the substation connecting two utilities. 40

4.13	Unbalance components report for substation that connecting two utilities. . .	41
4.14	The first example results when an event occurs.	42
4.15	The first example reports of current unbalance components when an event occurs.	43
4.16	The second example results when a fault occurs.	44
4.17	The second example reports of current unbalance components when an event occurs.	45
5.1	The analysis of the impact of a fault through the distance	48
5.2	Comparison of computed values and IoVs from locations B, C, D, E	49
5.3	Comparison of symmetrical components from locations B, C, D, E	50

List of Tables

4.1	Corresponding values of harmonics for the first sample result.	37
4.2	Corresponding values of harmonics for the second sample result.	39

Chapter 1

Introduction

1.1 Introduction

In recent years, more and more smart devices are installed in power industries: Phasor Measurement Unit (PMU), Supervisory Control and Data Acquisition (SCADA), Digital Fault Recorder (DFR), smart meter etc. With these devices, supervision for the whole grid in office becomes possible, and engineers can utilize the data to achieve analysis, test, simulation and evaluation of the system. However at the same time, with the development of information technology, more data is collected and accumulated. In the industries, the real-time values are widely utilized to monitor the status of the substations, transmission lines and individual equipment, but the historical records are seldom used to accomplish researches.

As the rapid development of power grid, power quality problem has become a hot topic, and the historical data is the most critical factor to complete the analysis. There are already some data visualization examples in Dominion Energy: one-line diagram, equipment

dashboard and DFR dashboard etc. The one-line diagram presents not only the layout of the grid, but also the real-time values for voltage, current and power. The equipment dashboard helps engineers monitor the status for individual equipment inside the substation. And the DFR dashboard contains all the DFRs in the transmission system, which helps fault analysis group identify and troubleshoot an event.

Because the success of those data visualization tools, a new dashboard that displays the data as well as analysis reports related to power quality problems is developed in this thesis. The data that utilized to accomplish the research is from digital fault recorders, and all DFRs is mapped in a google map. Three power quality issues - voltage and current variation, harmonics, voltage and current imbalance - are presented in the paper. By applying JavaScript and some web tools, the power quality dashboard is achieved as a web page so that everyone who has permission can access to it.

In the future, protection engineers can monitor the events with the dashboard, and troubleshoot the possible causes. Meanwhile, the gradient mapping can be also achieved to analyze the harmonic flows with a global trigger.

1.2 Outline of The Thesis

For the rest of the thesis, chapter 2 introduces related background and acknowledgement of power quality, DFRs and data visualization in power systems. The detail design of the dashboard is stated in chapter 3, including motivation, methods that utilized to accomplish the analyses and the web page design steps. Chapter 4 presented the interface layout for the dashboard as well as the analysis for each case of the result. In the end, the conclusion and future work is included in the chapter 5.

Chapter 2

Background and Related Acknowledgment

2.1 The Importance of Power Quality

2.1.1 Definition of Power Quality

In electric utilities, power quality can be defined in different ways depending on one's frame of reference. For example, reliability can be used as the definition of power quality in a utility, and the utility can demonstrate that its system is more than 99 percent reliable with the statistic results. An equipment manufacturer may define power quality as those characteristics of power supply that enable the equipment to work properly. And these characteristics may vary from different criteria. In this article, the definition of power quality is cited from book[1]: *"Any power problem manifested in voltage, current or frequency deviations that results in failure or inappropriate operation of customer equipment."*

However, just like quality in other goods and services, power quality is still difficult to quantify. No widely accepted definition of power quality exists. There are standards for voltage, current, frequency and other measurements, but the final criteria of power quality are defined by the performance of end-user equipment. If the power is not adequate for those needs, the quality is lacking[1]. In this paper, the common term for describing the subject is power quality. However, it is in fact voltage and current quality that is being utilized in all the cases.

The power quality events include but not limited to a) transients, b) voltage and current variations, c) voltage and current imbalance, d) harmonics and e) frequency variation[2]. Transients can be generated on the serving utility and propagate down to the end-user. There are two general categories of transients: impulsive and oscillatory, which reflect the waveform of a voltage or current. Variation can be classified to long-duration voltage variation and short-duration variation. If the root-mean-square deviations sustain longer than 1 minute, the variation is considered to be long-duration. The long-duration variations can be either over-voltage or under-voltage. The short-duration variations usually occur when there is a fault. To energize the large loads, it required high starting currents or intermittent loose connections in power wiring. Based on the fault location and system conditions, the fault can cause temporary voltage drops (sags), voltage rises (swells) or loss of voltage (interruptions). Voltage/current imbalance (also called voltage/current unbalance) is defined according to IEEE 112-1991: *the maximum deviation from average phase voltage, referred to the average of the phase voltage*. In recent standard IEEE std.936, the unbalance is defined as the ratio of negative and positive sequence voltage[3]. Harmonic distortions are deviation from ideal sinusoidal voltage or current wave of frequency characterized by the spectral content of the deviation. The distorted waveform can be decomposed into sum of the fundamental frequency and harmonics. Power frequency variation is defined as the deviation of the

fundamental frequency from the nominal frequency. It is usually related to the rotational speed of the generators that supply the systems. In this thesis, voltage and current variation, harmonic contents, voltage/current imbalance are analyzed and presented in a dashboard.

2.1.2 The Importance of Power Quality

The most essential reason that people care about power quality is economic issues. In industries, power quality has direct economic impact on the performance of the equipment and in some instances, the source of harmonics. With the development of the intelligent technology, there are more and more automation equipment, which means this electronically controlled, energy-efficient equipment is usually more sensitive to the deviation of the supplying voltage. Besides, electric utilities are also concerned about the power quality issues. In such a competitive environment, it is extremely important to meet the customers' expectation. There can be a significant economic impact on a utility if it loses disgruntled consumer to a competing power suppliers. Although residential users may not suffer from financial loss directly, they might transfer to another utility when they are provided poor power service. With the increasing usage of home electrical devices, especially computer, people become more sensitive to the interruptions. As a result, electric utilities are no longer just providing power to turn lights on or start the motors. Only high power quality can ensure the utility stand out in such a fierce competing environment.

2.1.3 Power Quality Evaluation Procedure

Power quality problem has large variety of phenomena, and each of phenomena may have wide range of causes and corresponding solutions. Figure 2.1 presents a set of general steps for a power quality evaluation[1].

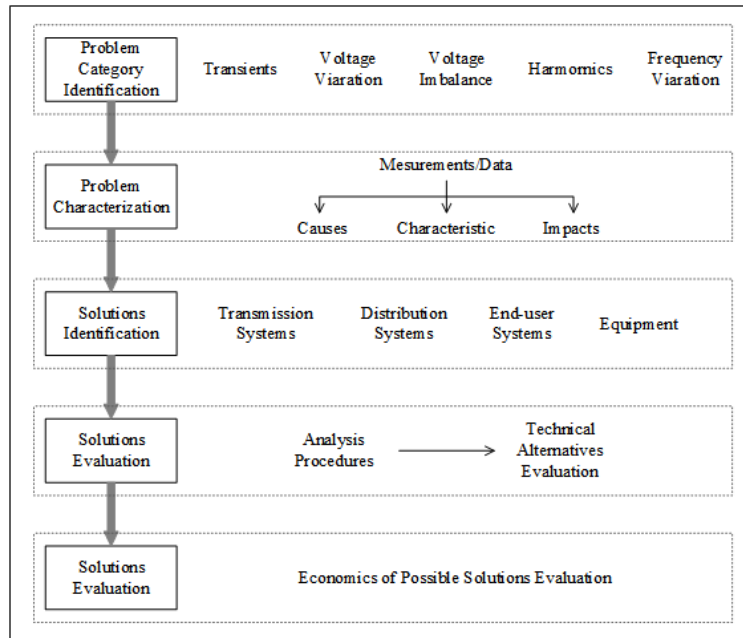


Figure 2.1: Steps of a power quality evaluation.

Engineers must identify what category of the problem as the very first step. After retrieving measurements/data from corresponding devices, the possible causes, characteristics and impacts can be analyzed out. Measurements play a critical role for almost any power quality problem. It is the essential element of the process to characterize the problems and the existing systems. Based on the analysis result from the problem, a variety of solutions can be proposed. Those solutions need to be evaluated with a system perspective, and both the economics and technical limitations must be taken into consideration.

2.2 Digital Fault Recorders (DFRs)

2.2.1 Definition

Fault recorders are one of the most important devices that protection engineers can have during the event investigation. They can provide the reasons for equipment failure, status of the equipment behavior during a fault or an event, and even the records that can be analyzed for the post-fault event. Nowadays, fault recorders are captured by microprocessor relays. However, the records are limited due to the sampling rate and the record length. The appearance of digital fault recorders solved those problem. They offer outstanding sampling rate, record length and unfiltered record capability[4]. DFRs are extremely useful in a utility, and the purposes of DFRs are stated as follows:

- DFRs can record power systems events, including faults, time of the fault, system disturbances or swings and abnormal instrument transformer behavior, such as current transformer (CT) saturation, DC offset, Ferro resonance etc.
- The protection system performance can be monitored through the fault records. With the measurements from DFRs, protection analysts can obtain information about the failure of a relay to operate, incorrect trip of system elements during faults, determination of optimum line reclose relay and failure of fault interrupting devices.
- Engineers can check the difference between measured values and calculated values in order to determine possible inconsistencies.
- Symmetrical components can be calculated from measured data, which can help adjust relay setting.
- By requiring historical measurements, analysts can analyze power quality through

wide range of related algorithms or simulations.

2.2.2 COMTRADE Standard

With the development of the information technology (IT) and the broad utilization of the communication media in power systems, more data is collected from different devices such as Phasor Measurement Unit (PMU), Supervisory Control and Data Acquisition (SCADA) and DFRs. These data are being used to accomplish the analysis, test, simulation, evaluation of the system and related protection schemes during a event. Since different device may have different data format, the formation of a common standard for data files is necessary. The common data format will facilitate the utilization of the proper data in a wide range of applications and help end-users of one system use the data from another system. Therefore, the new IEEE standard Common Format for Transient Data Exchange (COMTRADE) was formed by the IEEE PES Power System Relaying Committee[5].

According to COMTRADE standard, each record should contain four type of files: Header (. HDR) file, Configuration (.CFG) file, a binary data (.DAT) file and an optional Information (.INF) file. The header file is optional, and it's written by ASCII text, which is generated by the originator of the COMTRADE data, typically by using a word processor program. The creator can include any information in any order desire, such as location, source and data format etc. The configuration file is also an ASCII text file intended to be read by a computer program, so it must be saved in specific format. The following information should be included in the configuration file:

- Station name, identification of the device;
- Number of digital and analog channels;

- Channel names, units, and conversion factors;
- Line frequency;
- Sample rate;
- Initial time of the data;
- trigger time of the data;
- data file type;
- Time stamp multiplication factor.

The data file, written in ASCII or binary format, include all the transient measurements. And the information file contains extra information, which is readable to general user or a given class of user[6][7].

2.3 Data Visualization In Power Systems

2.3.1 Introduction of Big Data

Due to the development of IT, the growth of information causes data accumulation in many subject areas. There were 2.5 quintillion bytes of data generated daily in 2015, which is equivalent to a 2.5 million terabytes disk drive[8]. The biggest issue to process these data is the inadequacy of proper analytical methods, since their diversity needs human support of process of data analysis and high computational complexity of algorithms. Because of that, the analysis time is increased, hardware needs to be regularly updated, and the capability of distributed database should be improved. Those large and complex data which is being

difficult to process is also called big data. In traditional power industries, SCADA devices are helping grid operations at distribution level, and It can acquire 1.03 TB samples at 10000 inspection points. The advanced sensors nowadays such as PMU and smart meters can acquire 495 TB data also at 10000 points within one year. Besides the bloom of the power data, the number and variety of data sources are continuously increasing. Therefore, big data in power systems can be characterized as spatial-temporal and usually heterogeneous[9].

2.3.2 Data Visualization in Power systems

Due to the data explosion and the difficulty of processing these data, data visualization, a big data technology, has become a trend and been applied in power industries. For instance, in control center, there are real-time status on one-line diagrams, and engineers can identify the problems by supervising the value of voltage, current and flowing power. For another example, in transmission level, load flow is the one of the most important aspects for power system operation and planning. With the background processing of the real-time data and web designs, people sitting in the office can visually obtain the direction of power flows.

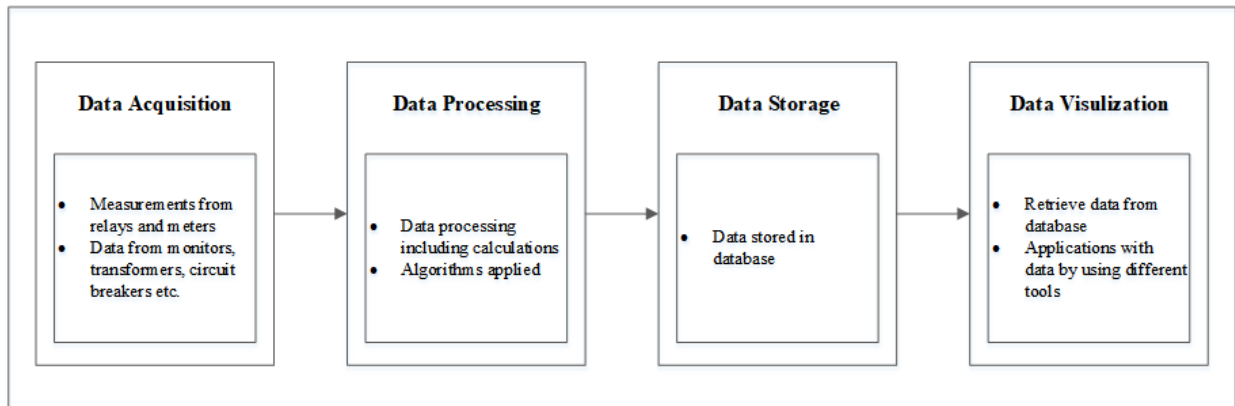


Figure 2.2: Procedures to realize data visualization.

There are four main stages to realize the data visualization. As presented in figure

2.2, all the measurements are collected locally from relays, meters or devices like monitors, transformers, circuit breakers etc. Through IEC61850 standard and communication devices, data, including voltage, current, frequency etc., will be transferred to a system operation center (SOC) and/or a regional operation center (ROC). These data can be utilized by reliability engineers for analyzing the load flow, state estimation and many other analyses to supervise the state, operation and the whole network. At the same time, the data is also stored in a database with large capacity. The historical data within months even years can be retrieved from the server, and be used for power quality analysis. A powerful database can also store the calculated data, such as real power, reactive power, harmonic contents etc., which is convenient for engineers to monitor the data. With these measurements or analysis outputs from the database and some software tools, data visualization can be accomplished.



Figure 2.3: An example of data visualization - DFR dashboard in Dominion Energy.

Figure 2.3 is an example of data visualization, which is a DFR dashboard from fault analysis group in Dominion Energy. The dashboard contains more than 200 DFRs in the transmission system, and it manages a massive amount of data. With the dashboard, people can monitor the real-time status for all DFRs. What's more, based on the warning signs,

engineers may be able to identify and troubleshoot the problems in time and prevent worse events.

Chapter 3

The Design of Power Quality

Dashboard

3.1 Motivation of The Project

Data visualization has become of great importance with the development of information technology and the data explosion in power systems. In Dominion Energy, there are already some applications developed and being utilized.

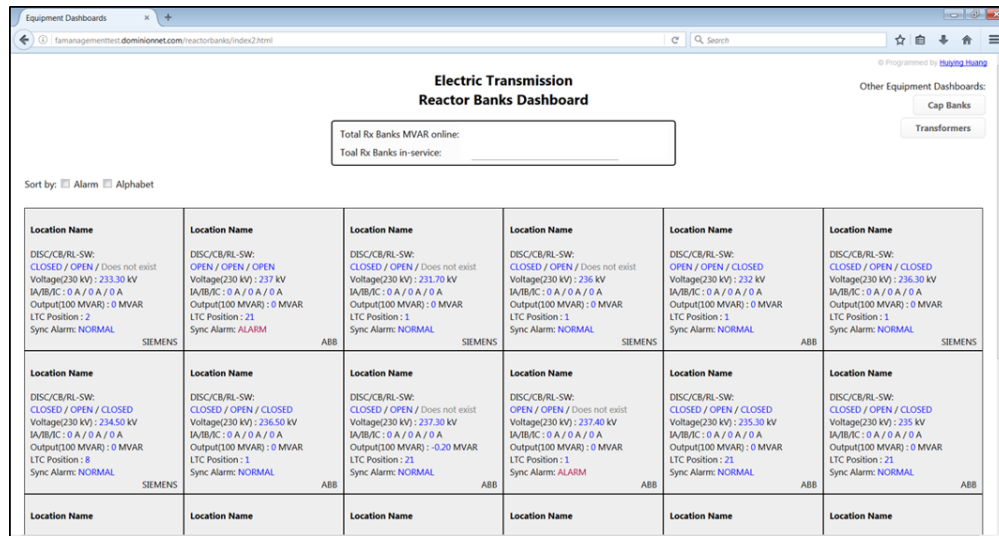


Figure 3.2: Reactor banks dashboard in Dominion Energy.

Figure 3.2 is the reactor banks dashboard in Dominion Energy. Besides the real-time measurements, engineers can also monitor different equipment in one web page and reduce unnecessary operations. For example, putting nearby reactor and capacitor banks in service at the same time may not be the optimal solution to achieve the end goal of the system operators. It is challenging to detect such situations without the visualization of data. However, engineers can now observe reactive power of reactor banks and capacitor banks to investigate when and why the operators or automatic controllers are operating them at the same time[10].

Due to the success of these data visualization applications in power industries, it is beneficial to develop similar tools in order to facilitate the grid reliability, system efficiency and reduce human errors. As introduced in chapter 2, digital fault recorders can not only capture events, but also record samples for voltage, current, frequency and other important operating parameters of the system. However, utilities seldom or sometimes never utilize these samples to analyze the power quality problems. When an event occurs, it is inevitable that voltage, current and frequency can be influenced, but many times, the signals might

indicate a condition leading to the fault. By analyzing the historical records in DFRs, it may be possible to determine the set of operating and/or equipment conditions that cause the fault. In addition to event analysis and possible prediction of faults, the work developed during this study can help to assess power quality problems and/or unbalanced operating conditions. The analysis includes:

- Voltage and current variations (sags and swells) from phasor estimation;
- Harmonic contents as well as how far these harmonics are spreading and how best to address them;
- Identify transmission assets being exposed to harmful levels of harmonics and respond accordingly;
- Unbalance components to evaluate the quality of power for interconnecting utilities.

In this paper, the analyses that have been completed are a) phasor calculation and the analysis from it; b) harmonic contents from the samples; c) unbalance components based on the records. Reports are generated after data processing and being displayed on a dashboard. The details of each analysis and the deployment of the dashboard will be stated later in this chapter.

3.2 Related Analyses for Power Quality Problems

3.2.1 Phasor Estimation

Estimation of voltage/current phasors is the essential method for power quality assessment. A phasor represents the magnitude and phase angle associated with a sinusoidal signal

with respect to a reference.

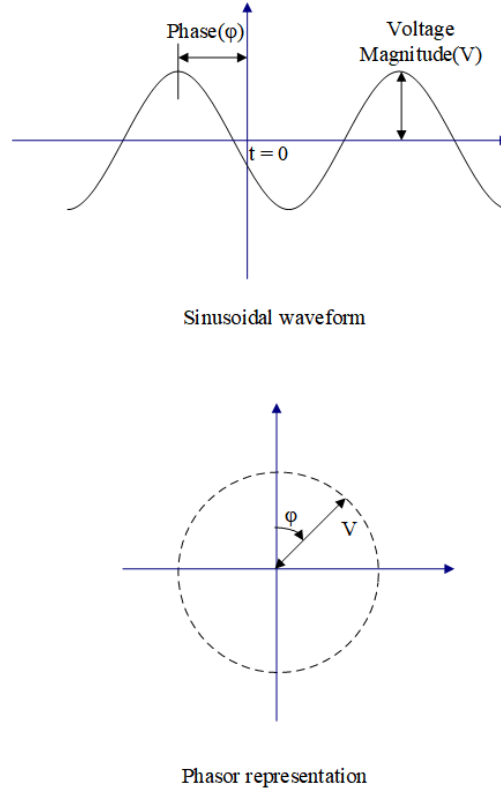


Figure 3.3: Sinusoidal waveform and its phasor representation.

Figure 3.3 illustrate the phasor representation. The length of the phasor is equal to the RMS value of the sinusoid. The phase angle is the distance between the signal's sinusoid peak and a specific reference, and is presented by an angular measure. The reference is a fixed point in time domain. The phasor magnitude is related to an amplitude of the sinusoidal signal[11].

Consider a pure sinusoid signal:

$$X(t) = X_m \sin(\omega t + \phi) \quad (3.1)$$

ω is the frequency of the signal in radians per second and ϕ is the phase angle in radians.

X_m is the peak value of the signal. Equation 3.1 can also be presented as:

$$X(t) = Re\{X_m e^{j(\omega t + \phi)}\} \quad (3.2)$$

It can be also represented by a complex number X known as its phasor representation:

$$X = \frac{X_m}{\sqrt{2}} e^{j\phi} = \frac{X_m}{\sqrt{2}} [\cos\phi + j\sin\phi] \quad (3.3)$$

To estimate the phasor for the signal, a recursive algorithm is applied in this project. Consider a constant input signal $x(t)$ at the nominal frequency of the power systems f_0 (usually $50Hz$ or $60 Hz$), which has sample rate of Nf_0 . N is the total sample number for each cycle. The sampling angle θ equals to $\frac{2\pi}{N}$, and the phasor estimation is presented as equation 3.4.

$$x(t) = X_m \cos(2\pi f_0 t + \phi) \quad (3.4)$$

The N samples of this signal x_n are:

$$x_n = X_m \cos(n\theta + \phi) \quad n = 0, 1, 2, \dots, N - 1 \quad (3.5)$$

Discrete Fourier transform (DFT) can be utilized to extract the fundamental components of the sample values:

$$X(k) = \frac{\sqrt{2}}{N} \sum_{n=0}^{N-1} x(n) [\cos(2\pi \frac{k}{N} n) - j\sin(2\pi \frac{k}{N} n)] \quad (3.6)$$

To find the magnitude and angle of the fundamental frequency signal associated with the

sampled values, k is set to a value of 1 in equation 3.6. The result is:

$$X(1) = \frac{\sqrt{2}}{N} \sum_{n=0}^{N-1} x(n) [\cos(\frac{2\pi}{N}n) - j\sin(\frac{2\pi}{N}n)] \quad (3.7)$$

Since $\frac{2\pi}{N} = \theta$,

$$X(1) = \frac{\sqrt{2}}{N} \sum_{n=0}^{N-1} X_m \cos(n\theta + \phi) [\cos(n\theta) - j\sin(n\theta)] \quad (3.8)$$

Apply the trigonometric identified for $\cos(a) \cdot \cos(b)$ and $\cos(a) \cdot \sin(b)$, the real component can be reduced to:

$$X(1)_{real} = \frac{\sqrt{2}X_m}{N} \sum_{n=0}^{N-1} [\cos(\phi) \cdot \cos^2(n\theta) - \frac{1}{2}\sin(\phi)\sin(2n\theta)] \quad (3.9)$$

$$X(1)_{real} = \frac{X_m}{\sqrt{2}} \cos(\phi) \quad (3.10)$$

Similar to the real component, the imaginary component can be represented as:

$$X(1)_{imag} = -\frac{\sqrt{2}X_m}{N} \sum_{n=0}^{N-1} x(n) [\cos(\phi) \cdot \sin(2n\theta) - \sin(\phi)\sin^2(n\theta)] \quad (3.11)$$

$$X(1)_{imag} = \frac{X_m}{\sqrt{2}} \sin(\phi) \quad (3.12)$$

The expression of the phasor reduces to the known phasor notation:

$$X(1) = \frac{X_m}{\sqrt{2}} ([\cos(\phi) + j\sin(\phi)]) = \frac{X_m}{\sqrt{2}} \cdot e^{j\phi} \quad (3.13)$$

If the phasor is computed from samples r to $r + (N - 1)$:

$$X^{N-1} = \frac{\sqrt{2}}{N} \sum_{n=0}^{N-1} x(r+n) \cdot e^{-jn\theta} \quad (3.14)$$

And the phasor calculated from samples $r + 1$ to $r + N$:

$$X^N = \frac{\sqrt{2}}{N} \sum_{n=0}^{N-1} x(r + 1 + n) \cdot e^{-jn\theta} \quad (3.15)$$

Equations 3.14 and 3.15 indicate that those 2 consecutive phasor estimations have $N - 1$ samples in common and that those common samples are multiplied by different factors. If the phasor is calculated from the first sample, where $r = 0$, the latest phasor can be expressed as

$$X^N = \frac{\sqrt{2}}{N} \sum_{n=0}^{N-1} x(n + 1) \cdot e^{-j(n)\theta} \quad (3.16)$$

Multiply $e^{-j\theta}$ on both side:

$$X^N \cdot e^{-j\theta} = \frac{\sqrt{2}}{N} \sum_{n=0}^{N-1} x(n + 1) \cdot e^{-j(n+1)\theta} \quad (3.17)$$

In this representation, the $N - 1$ common samples are multiplied by same factors as the last phasor X^{N-1} . Therefore, the latest phasor can also be presented as:

$$X^N \cdot e^{-j\theta} = \frac{\sqrt{2}}{N} \left[\sum_{n=0}^{N-1} x(n) \cdot e^{-j(n)\theta} - x(0) \cdot e^{-j(0)\theta} + x(N) \cdot e^{-j(N)\theta} \right] \quad (3.18)$$

$$X^N \cdot e^{-j\theta} = X^{N-1} + \frac{\sqrt{2}}{N} [x(N) \cdot e^{-j(N)\theta} - x(0) \cdot e^{-j(0)\theta}] \quad (3.19)$$

$$\bar{X}^N = X^{N-1} + \frac{\sqrt{2}}{N} [x(N) - x(0)] \cdot e^{-j(0)\theta} \quad (3.20)$$

where \bar{X}^N is a non-rotating phasor since the rotation can be corrected due to the sampling rate. When the last sample is $N + r$, as a function of the samples in the set finishing at $N + r - 1$, the general form of phasor is given by:

$$\bar{X}^{N+r} = \bar{X}^{N+r-1} + \frac{\sqrt{2}}{N} [x(N + r) - x(r)] \cdot e^{-jr\theta} \quad (3.21)$$

The recursive algorithm utilizes the previous phasor and only 2 of the samples - the latest one the first one in last cycle to evaluate the new phasor.

After the fundamental phasor values are computed, the sample values, acquired from the time-domain signals in the field, can be estimated for each moving window (cycle):

$$x_{est}(r+n) = \sqrt{2} \cdot |\bar{X}|^{N+r} \cdot \cos[(r+n) \cdot \theta + \phi] \quad n = 0, 1, 2, \dots, N-1 \quad (3.22)$$

where $|\bar{X}|^{N+r}$ is the absolute value of the fundamental value.

In this paper, Index of Variance (IoV) for each cycle is applied to decide whether or not perform the next step of analysis. Define the deference between collected value and calculated value as following:

$$iov(n) = |x(n) - x_{est}(n)| \quad (3.23)$$

And a recursive formula can also be utilized to calculate the IoV:

$$IoV^{N+r-1} = \frac{1}{N} \sum_{n=0}^{N-1} iov(n+r-1) = \frac{1}{N} \sum_{n=0}^{N-1} |x(n+r-1) - x_{est}(n+r-1)| \quad (3.24)$$

$$IoV^{N+r} = IoV^{N+r-1} + \frac{1}{N} [iov(N+r) - iov(r)] \quad (3.25)$$

The calculated IoV can be used to assess the possible nature of the event. If the index grows or decays in a short period of time, the event can be considered a switching event or a fault. On the other hand, IoV lasting a long period (several cycles) may be associated with harmonic or power quality events. For instance, if the IoV sustains for 0.5 cycle to 1 minute, it might be a sag or a swell[1]. The detail discussion will be presented in the next chapter.

3.2.2 Harmonic Contents

In the recent years, the wide application and use of power electronic has resulted in a deterioration of power quality in power systems. Therefore, the research and analysis of harmonics of voltage and/or current has become popular. There are three main reasons for harmonics: a) non-linear load; b) Power supply; c) harmonic produced by transmission and distribution systems[12]. But the non-linear load is the most common and important reason.

One of the characteristics of non-linear loads is that the current is not proportional to the applied voltage, and as a result harmonics are created in the circuit. To evaluate and analyze the harmonic contents in the signal, Fast Fourier Transform (FFT) method is utilized in this thesis. FFT is an efficient algorithm for the evaluation of Discrete Fourier Transform (DFT), and it computes the DFT of a sequence. Therefore, the fundamental mathematical operation is DFT. It is implied from Fourier Transform (FT) that any periodic signal can be represented by an infinite sum of sine and cosine terms:

$$X(\omega) = \int_{-\infty}^{\infty} x(t) \cdot e^{-j\omega t} dt \quad (3.26)$$

And the Discrete Fourier Transform is an application of Fourier transform (FT) to discrete signal for determining harmonic and frequency contents of discrete signal. Equation 3.27 is the formula of DFT, where: 1) k represents the k^{th} harmonic frequency; 2) n is the time domain index of the sample input signal and 3) N is the total number of the samples.

$$X(k) = \frac{2}{N} \sum_{n=0}^{N-1} x(n) \cdot e^{-j2\pi \frac{k}{N} n} \quad (3.27)$$

Applying Eulers Identity, equation ?? above can also be written as:

$$X(k) = \frac{2}{N} \sum_{n=0}^{N-1} x(n) [\cos(2\pi \frac{k}{N} n) - j \sin(2\pi \frac{k}{N} n)] \quad (3.28)$$

When $k = 1$, $X(1)$ represents the fundamental component of the sampled signal assuming that the summation is over the whole period of the fundamental frequency.

When processing the signal, aliasing may appear due to the overlap of frequency regions in the spectra. Figure 3.4 is the spectrum of a band-limited signal with spectral overlap. If the bandwidth f_0 is larger than half of the sample frequency f_s , the aliasing phenomenon occurs.

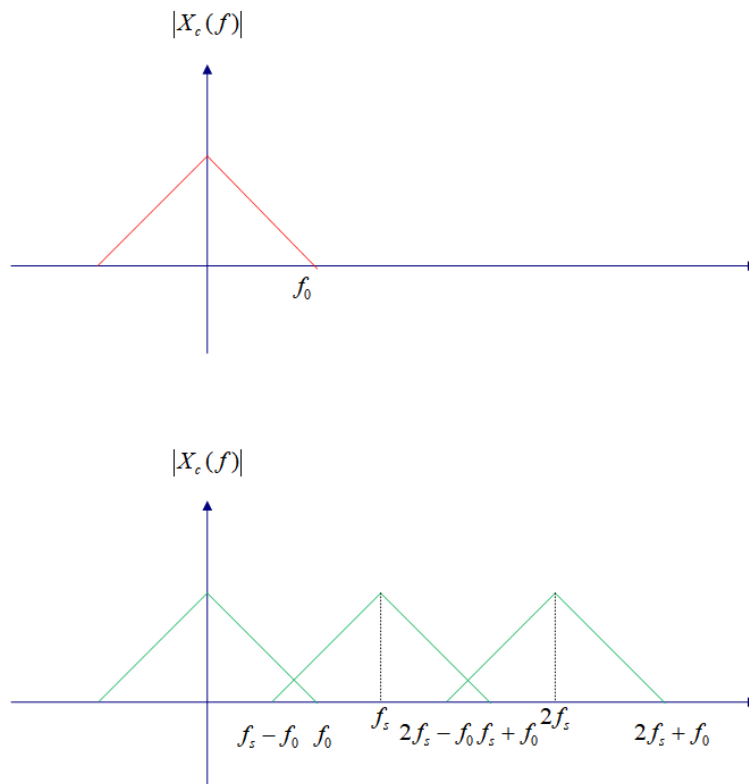


Figure 3.4: Spectrum of a band-limited signal with spectral overlap.

Therefore, in order to recover the original signal from the sampled data, Nyquist sam-

pling theorem is applied. According to it, *The sampling frequency should be at least twice the highest frequency contained in the signal.* Or in mathematical terms[13]:

$$f_s > 2f_0 \quad (3.29)$$

It is indicated that to analyze the harmonic contents, the highest frequency should be less than half of the sampling rate:

$$f_0 < \frac{1}{2}f_s \quad (3.30)$$

As a result, in this project, the highest harmonic that processed is lightly smaller than half of the sample frequency.

3.2.3 Imbalance Components

In a balanced power systems, with only linear loads connected to the system, the phases of power supply are 120 degrees apart in terms of phase angle and magnitude of peaks should be the same. Unbalance is any deviation in either voltage/current magnitude or angle displacement between phases. The following aspects may result in voltage or current imbalance: a) a three phase equipment (for example, induction motor) with a damage winding would result in a unbalance in its winding; b) large single phase load; c) switching of three-phase heavy loads; d) unequal impedance in power transmission or distribution systems[14]. Even minor imbalance can cause serious consequences. It may reduce motor/equipment efficiency, and result in unnecessary trip, increasing loses, even permanent damage. Consequently, voltage or current imbalance is a problem that should not be neglected.

To analyze the unbalanced conditions, it is necessary to evaluate the symmetrical components of the original system. By using the equations 3.15 and 3.21, the fundamental values

for each phase can be calculated:

$$\overline{X}_a^{N+r} = \overline{X}_a^{N+r-1} + \frac{\sqrt{2}}{N} [x_a(N+r) - x_a(r)] \cdot e^{-jr\theta} \quad (3.31)$$

$$\overline{X}_b^{N+r} = \overline{X}_b^{N+r-1} + \frac{\sqrt{2}}{N} [x_b(N+r) - x_b(r)] \cdot e^{-jr\theta} \quad (3.32)$$

$$\overline{X}_c^{N+r} = \overline{X}_c^{N+r-1} + \frac{\sqrt{2}}{N} [x_c(N+r) - x_c(r)] \cdot e^{-jr\theta} \quad (3.33)$$

where \overline{X}_a^{N+r-1} , \overline{X}_b^{N+r-1} , \overline{X}_c^{N+r-1} are previous computed phasors.

Define a phasor rotation operator α , which rotates a phasor vector counterclockwise by 120 degrees:

$$\alpha = 1\angle 120^\circ \quad (3.34)$$

Therefore,

$$\alpha^2 = 1\angle 240^\circ \quad (3.35)$$

So the A matrix utilized to transform the sequence values to phase values is:

$$A = \begin{bmatrix} 1 & 1 & 1 \\ 1 & \alpha^2 & \alpha \\ 1 & \alpha & \alpha^2 \end{bmatrix} \quad (3.36)$$

The transformation is presented as:

$$\begin{aligned}
 X_{abc} &= \begin{bmatrix} X_a^n \\ X_b^n \\ X_c^n \end{bmatrix} \\
 &= \begin{bmatrix} 1 & 1 & 1 \\ 1 & \alpha^2 & \alpha \\ 1 & \alpha & \alpha^2 \end{bmatrix} \cdot \begin{bmatrix} X_0^n \\ X_1^n \\ X_2^n \end{bmatrix} \\
 &= X_{012}
 \end{aligned} \tag{3.37}$$

Thus, the sequence components are derived from:

$$X_{012} = A^{-1} \cdot X_{abc} \tag{3.38}$$

where

$$A^{-1} = \frac{1}{3} \cdot \begin{bmatrix} 1 & 1 & 1 \\ 1 & \alpha & \alpha^2 \\ 1 & \alpha^2 & \alpha \end{bmatrix} \tag{3.39}$$

As a result,

$$X_{012} = \begin{bmatrix} X_0^n \\ X_1^n \\ X_2^n \end{bmatrix} = \frac{1}{3} \begin{bmatrix} 1 & 1 & 1 \\ 1 & \alpha & \alpha^2 \\ 1 & \alpha^2 & \alpha \end{bmatrix} \cdot \begin{bmatrix} X_a^n \\ X_b^n \\ X_c^n \end{bmatrix} \tag{3.40}$$

According to standard IEEE Std.1159, the unbalance factor, which is the ratio of negative sequence and positive sequence, is utilized to characterize the voltage and/or current imbalance.

$$UF = \frac{X_2}{X_1} \tag{3.41}$$

In order to analyze causes for an event, the ratio of zero sequence value and positive sequence value is also presented in the result.

$$UF_0 = \frac{X_0}{X_1} \quad (3.42)$$

3.3 Dashboard Design

To achieve data visualization, some tools are needed. In many instances, OSIsoft PI, SAS platforms and Grafana Labs are utilized to display data. However, those platforms have some limitations: they are hard to maintain and may lack flexibility. They might have some excellent features but can't satisfy all needs as the project is moving on and more functions may be needed. Besides, when automatic updates are demanded, it is impossible to accomplish it with these platforms.

Therefore, in this project, JavaScript, a high-level programming language, and some web development tools are applied to build up a website to display the analysis results. With this method, it is easier to add or change features of the dashboard, and there is no need for engineers to install any extra software. What's more, human effort can be reduced once the framework done.

There are 6 stages to develop a web application: information gathering; planning; design; development, testing and delivering; maintenance[15]. In this paper, the first five stages are presented in this section, the last stage will be included in the future work.

1. Information Gathering

The first step to build a success web page is to gather information. It is also the most important stage since it involves a solid understanding of the end-user. The following

things are taken into consideration:

- Purpose: provide power quality information to the engineers in order to troubleshoot the problems quickly and be able to predict events in the future.
- Goals: map DFRs in a Google map, and present all the analytical results of a selected DFR in subsequent page. User can select a specific unit by double-clicking over the graphical display.
- Target audience: engineers in protection and transmission group.
- Content: the mapping of all the sample DFRs, power quality and symmetrical component report for each of them.

2. Planning

In this stage, the detail algorithm and the tools as well as methodologies are determined. For this project, recursive algorithm, Fast Fourier Transformation and symmetrical component transformation are applied to analyze the data collected from the field. All data output is stored in a CSV file and will be moved to a database in the future. In the front page, the results are retrieved by using JavaScript, and interface was developed by using HTML5 as well as other web tools such as Vue.js, Chart.js etc.

3. Design

The prototype design is carried out from this step. Since the application is designed for engineers, the interface should be clean and the functions can't be complicated. In this project, the starting page is a map with clearly identifiable of field-installed DFRs. After double clicking a selected unit, a new tab will appear, and in this page, the comparison and IoV between collected values and computed values will be displayed as default. Menus are used to switch to another two analyses.

4. Development

The development stage is the point where the application itself is created.

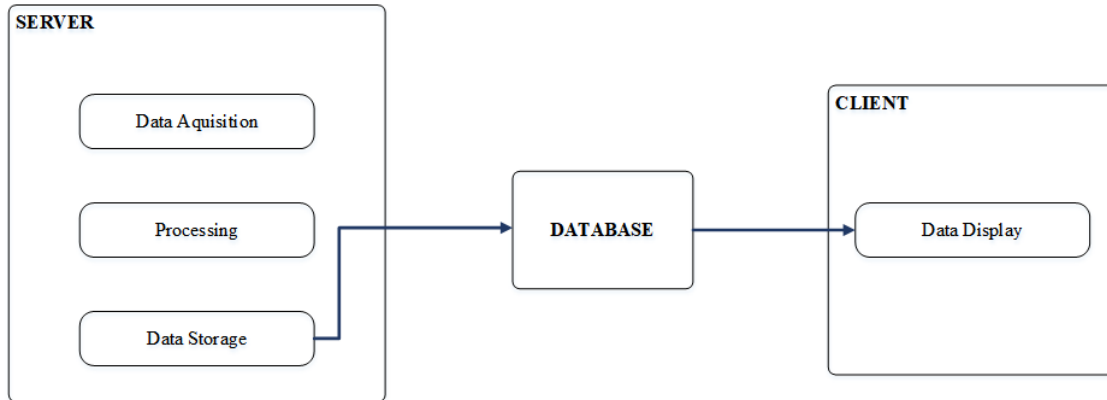


Figure 3.5: Procedure of data server-client application implementation.

Figure 3.5 shows the structure of data-server-client application implementation. In the SERVER, a) measurements are acquired from DFRs; b) data is processed using the analysis methods stated in Chapter 3; c) original measurements and information results are stored in a database. In this project, a CSV file is used since the sample data is not large. A future implementation of this last step will include a DATABASE with all original samples and results. In the CLIENT part, data is retrieved from database and displayed through the web page.

5. Testing and Delivery

When the framework is completed, the test of the application is needed. During the development of this work, seven data spreadsheets from different field-installed DFRs are utilized to test and verify the adequacy of the dashboard. The mapping of these seven locations was initially tested, followed by the display of data to verify accuracy and correctness. Since this project is at its initial stage and still under development, the upload for the website will be accomplished in the future.

Chapter 4

Results and Case Study

4.1 The Details of Power Quality Dashboard

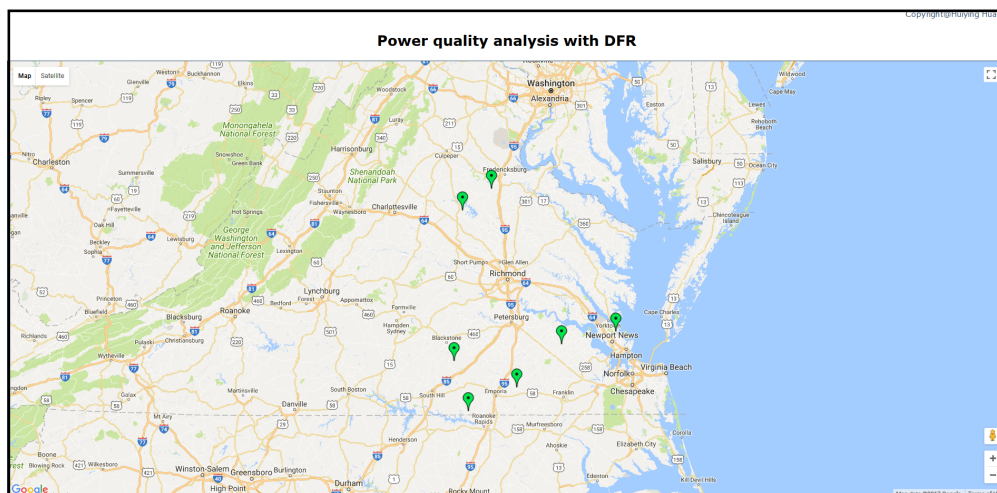


Figure 4.1: The start page of power quality dashboard.

As mentioned in last section, the starting page of the power quality dashboard is a Google map with DFR location markers. In this project, as the first step into developing a complete system display, there are seven DFRs to be used for testing. The green markers in

figure 4.1 mark the locations for the test digital fault recorders.

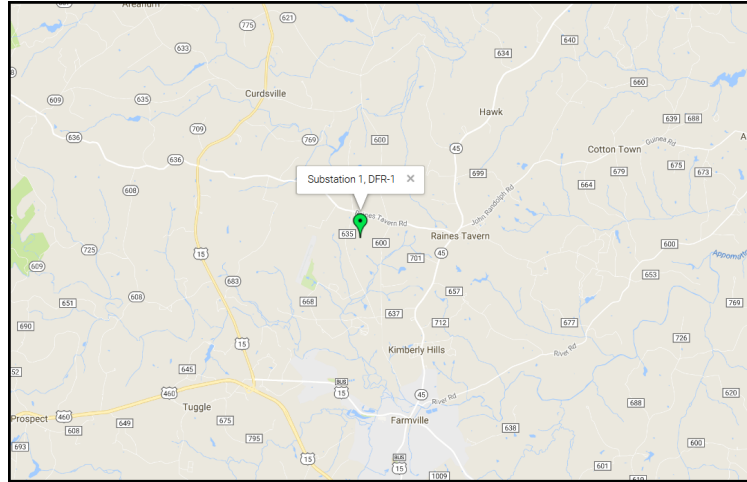


Figure 4.2: DFR Information will be displayed when the marker is clicked.

When the marker is clicked, the map will be zoomed in and centered at the location. Meanwhile, the substation name and DFR number will be displayed as shown in figure 4.2.



Figure 4.3: The marker will link to a report page after double clicking it.

Double-clicking the marker will create a report page as shown in figure 4.3. In this page, the substation name and DFR number related to the marker is under the title. The initial

figure includes the original sampled values as well as the values calculated by the fundamental phasor approximation obtained from the DFT. With these two values as inputs, the Index of Variance is calculated from equation 3.24. Both voltage and current are presented in the analysis report as shown in figure. The menu can be switched to display harmonic contents report or unbalance components report. Since the records are from the transmission level of a highly interconnected system, the voltage is mostly constant in frequency and magnitude; it rarely displays variations due to harmonics or unbalanced conditions. As a result, in this project, only the current harmonics and current unbalance components are included in the dashboard. If in the future a similar dashboard is built for distribution level, harmonic and imbalance analyses must be included for both voltages and currents.

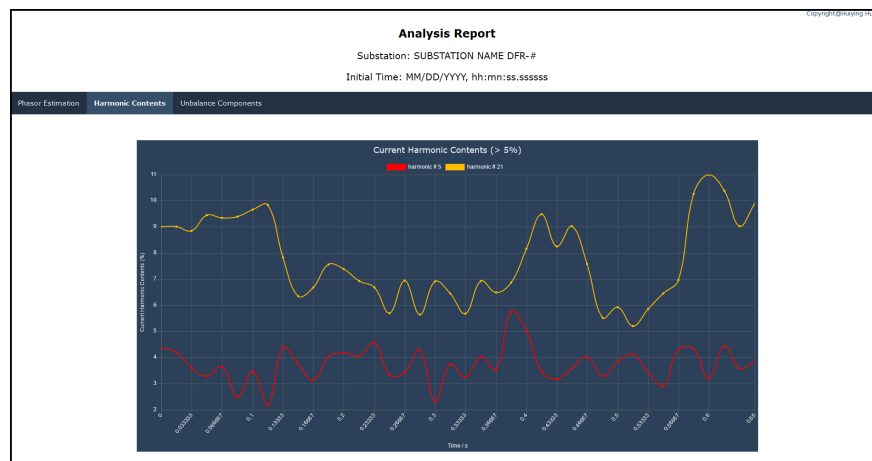


Figure 4.4: Current harmonic contents report page.

Figure 4.4 is the layout of the harmonic contents report page. The graph plots the harmonic contents as a function of time. Harmonic components with at least 5% (this is a user-adjustable value) of the fundamental value are displayed.

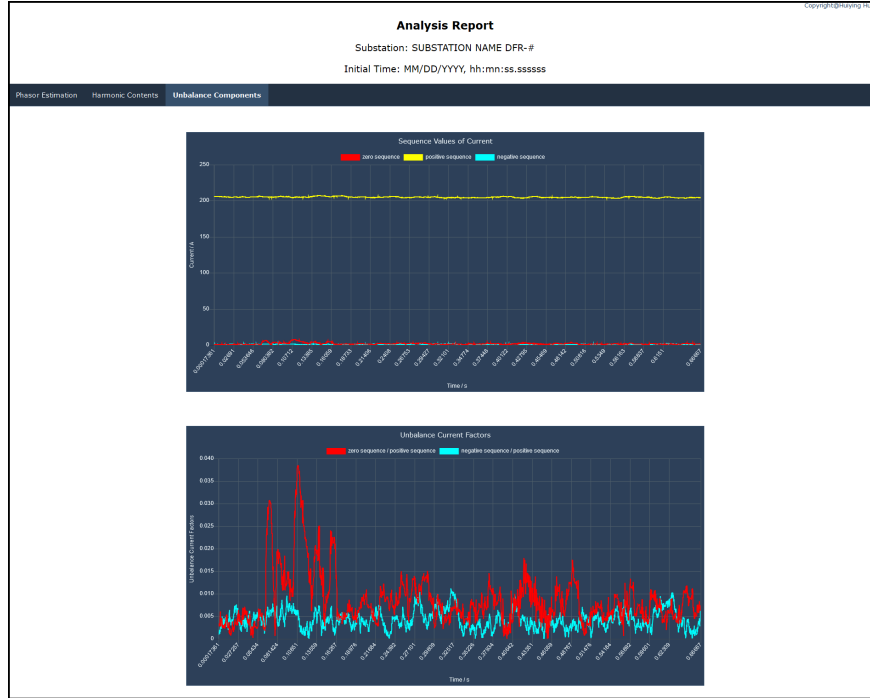


Figure 4.5: Current unbalance report page.

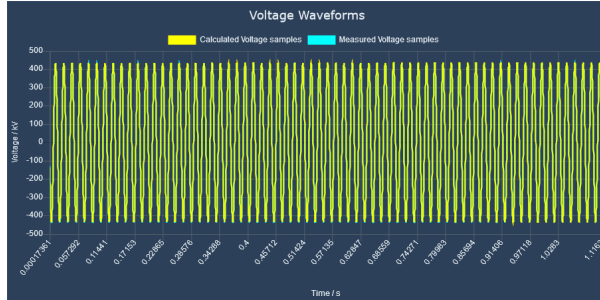
Figure 4.5 is a sample current unbalance components report page. The page is separated into two parts: the first part shows the value of the sequence component current over time, which can help engineers to determine the possible reason of a fault quickly. The second graph presents the unbalance current factors versus time. The ratio of negative sequence against positive sequence and the ratio of zero sequence against positive sequence is plotted in the chart. According to IEEE standard 519, there might be an unbalanced condition in a transmission system when the ratio is higher than 0.05.

4.2 Case Study

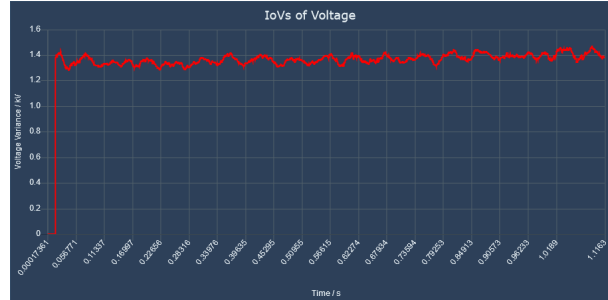
In this section, three possible case reports will be analyzed and presented as following: a normal report without event, reports that contain harmonics and reports that have unbalance

issue and fault analyses based on unbalanced conditions.

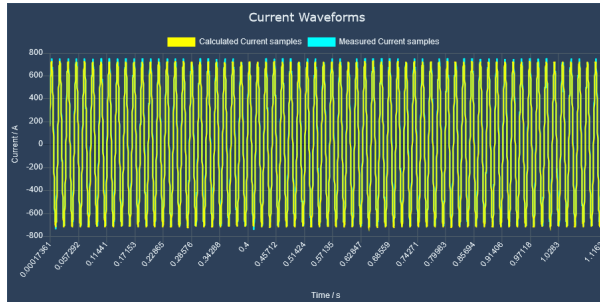
4.2.1 Normal Result Without Power Quality Issue



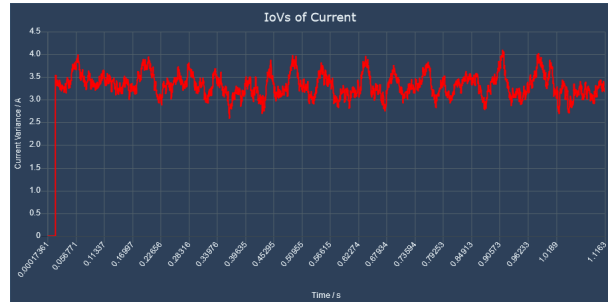
(a) Phasor estimation for voltage



(b) IoVs of voltage



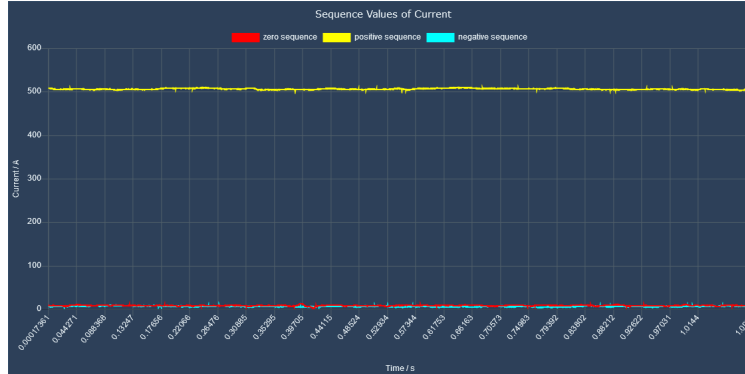
(c) Phasor estimation for current



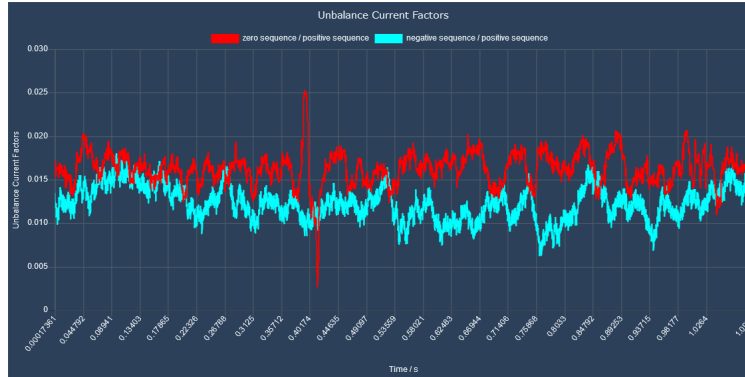
(d) IoVs of current

Figure 4.6: Normal report of phasor estimation without power quality issue.

Figure 4.6 is the phasor estimation report from a traditional substation that has no power quality issue. From the chart, it can be seen that the collected values and computed values are almost overlapping for both voltage and current. And the average errors of voltage are stabilized at 1.4, which is small. The average errors of current are fluctuated but within the threshold value of 5 amps. For this situation, the server will not calculate the harmonic contents as the maximum value doesn't exceed the threshold value. Therefore, no harmonic reports will be shown in the harmonic contents page.



(a) Sequence values of current.



(b) Current unbalance factors.

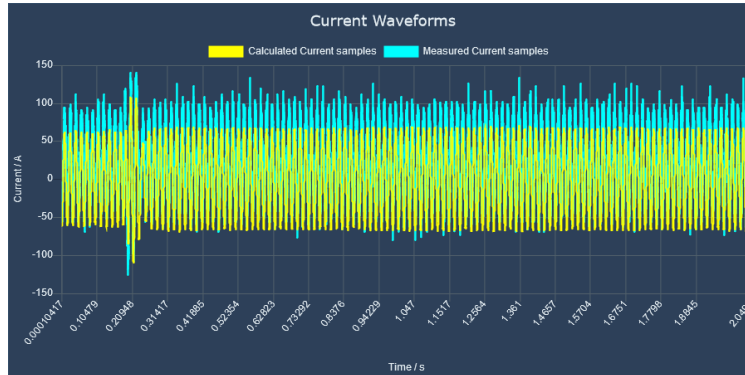
Figure 4.7: Normal report of current unbalance components without power quality issue.

The unbalance components report is shown in figure 4.7. It can be referred from figure 4.7a that the zero sequence values and the negative values are around zero. The positive values are about the same as RMS value of the phase current. As for the unbalance factors (figure 4.7b), both of them are below 0.05, so there is no imbalance issue.

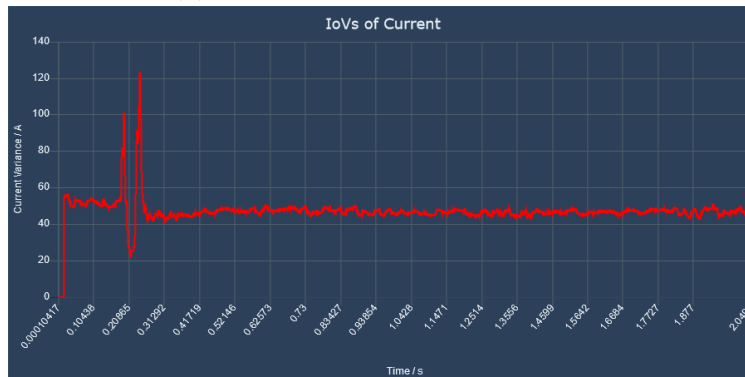
4.2.2 Results For Harmonic Contents

The main analysis for harmonic contents in this paper is from the substation that connected to solar generators. When the solar generators generate more power in the morning, the voltage harmonics are unchanged as mentioned in last chapter. But the current harmon-

ics can be more, depending on the supplied power and type of load. During the night time, the solar panels stop to generate power but receive power from the grids. At the same time, they provide reactive power to the grid, which can create noise[16]. As a result, the server initialized the harmonics analysis based on the IoVs from current.



(a) Phasor estimation for current



(b) IoVs of current

Figure 4.8: Reports of phasor estimation for a substation connected to a solar generator.

First sample result is from a record that was initialized in the early morning before sunrise. Figure 4.8 presents the current phasors and IoVs between collected values and calculated values. From 4.10, it can be observed that the IoVs are all higher than 40 amps and stabilized at around 48 amps except the event between 0.185 second and 0.255 second. Therefore, the IoVs triggered the harmonic analysis from the beginning to the end.

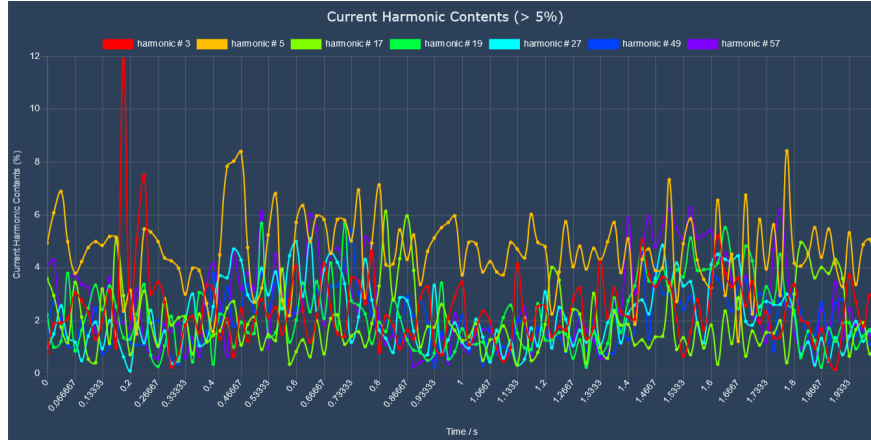


Figure 4.9: Harmonic contents against time for substation connected to a solar generator.

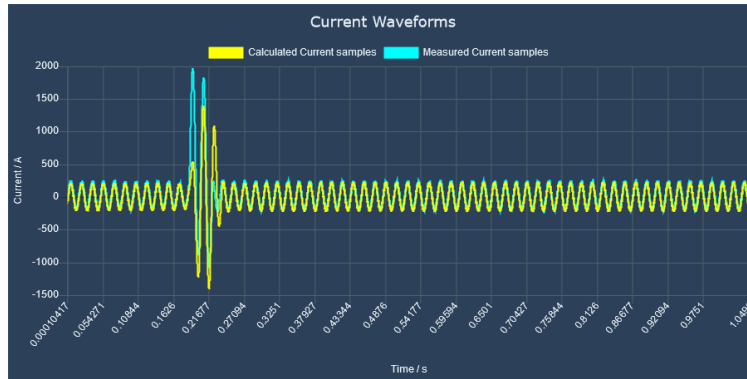
Figure 4.9 is harmonic analysis result over time. It can be seen from the chart that at some points, 3rd, 5th, 17th, 19th, 27th, 49th, 57th harmonics are larger than 5%. Table 4.1 is the corresponding values of current harmonics presented in figure 4.9 during the first 0.1 second. When an event occurs at 0.185 second, the 3rd harmonic starts to fluctuate and then return back to normal after 0.255 second.

Table 4.1: Corresponding values of harmonics for the first sample result.

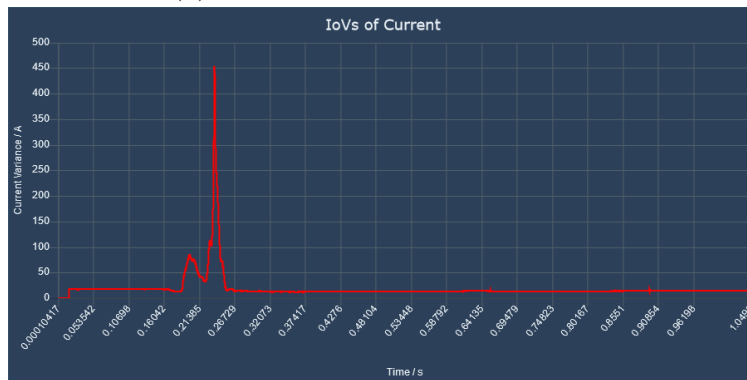
time	1st	3rd	5th	7th	17th	19th	49th	57th
0	61.283	0.48995	3.0277	0.14379	2.1973	1.3721	0.86043	2.5197
0.016667	60.829	1.1573	3.6897	0.36858	1.7864	0.60534	1.6415	2.6151
0.033333	63.129	1.2162	4.339	0.8237	1.107	0.777	1.281	1.0587
0.05	61.465	1.2748	3.0656	1.3153	0.71309	2.3311	0.67033	2.1586
0.066667	61.543	1.861	2.3271	0.52023	2.1171	0.53074	0.6157	2.2949
0.083333	59.724	1.6515	2.5281	0.9435	1.2752	0.9737	1.1567	2.0158
0.1	61.516	1.4107	2.9361	0.61824	0.3467	1.5316	0.86914	2.0014

Second example is the record that was initialized at noon. Figure 4.10 is its phasor estimation result. Except the event from 0.18 second to 0.25 second, the IoVs are not as

high as the first sample result but still exceed the threshold value (they are stabilized at about 13). Therefore, the server analyzes the harmonics for the whole 1 second.



(a) Phasor estimation for current



(b) IoVs of current

Figure 4.10: Second reports of phasor estimation for a substation connected to a solar generator.

The harmonics report for this sample is shown in figure 4.11, and corresponding values for first 0.1 second is presented in table 4.2.

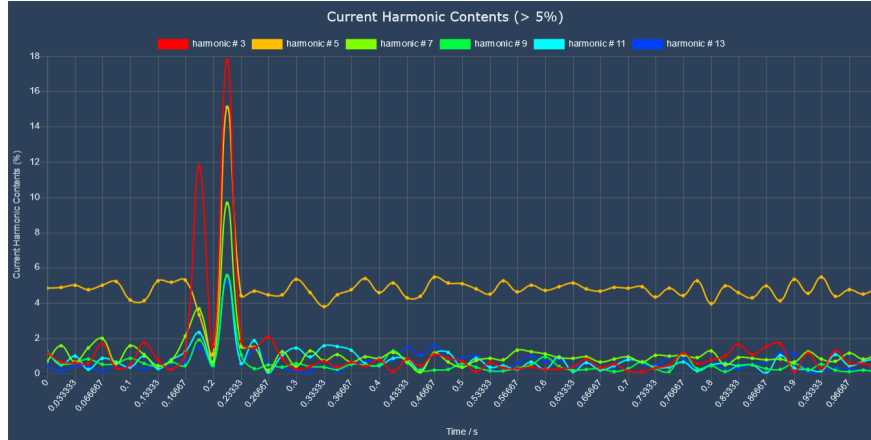


Figure 4.11: Harmonic contents for the second result.

There is no high harmonics such as 49th and 57th harmonic in the first example, and the largest one extracted from the sample data is 13th harmonic. Besides, the harmonic contents are much more stable than the first result. The 5th harmonic is stabilized at around 10 amps as shown in table 4.2. The same as the first result, when a event occurs, the harmonics are going up for a short amount of time and return back to normal after the fault has been cleared.

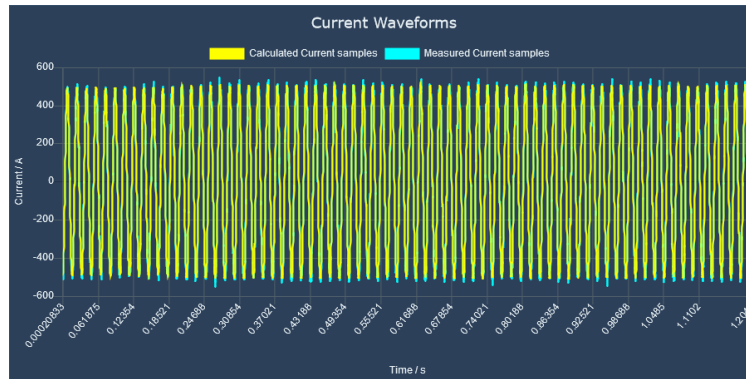
Table 4.2: Corresponding values of harmonics for the second sample result.

time	1st	3rd	5th	7th	9th	11th	13th
0	205.28	2.4301	9.9691	1.4333	2.5189	2.5544	0.84131
0.016667	204.8	1.336	10.048	3.2633	1.2087	1.0413	0.3425
0.033333	205.54	1.239	10.296	1.398	1.2916	2.0409	0.91942
0.05	205.17	1.1696	9.7793	3.0261	1.6738	0.48773	0.7479
0.066667	204.79	3.4728	10.301	4.1278	1.079	1.7656	0.25012
0.083333	204.62	0.6698	10.688	1.1811	1.1702	1.3759	1.1277
0.1	205.29	0.97627	8.6103	3.2142	1.7412	0.73883	0.83858

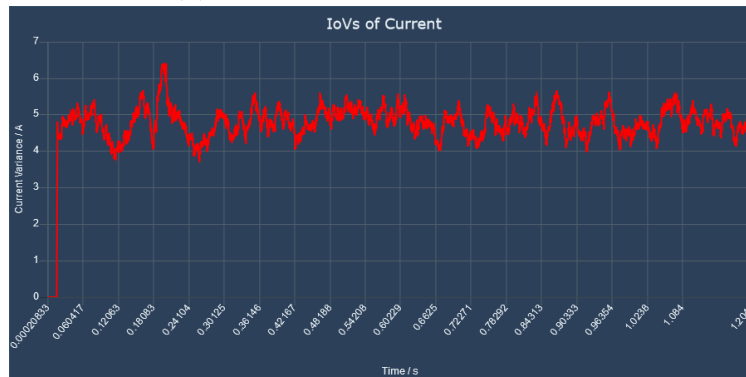
From these two sample results, it can be concluded that the solar generators produce more harmonics during the nighttime than in the daytime. Meanwhile, the harmonics become more stable when the generators generate power and inject to the power grids.

4.2.3 Results For Unbalance Components

Different utilities use different voltage standard to transmit the power. And they don't transpose the phase voltages when transmitting extra high voltage (usually larger than $345kV$). Due to the different reactance in different lines, the current imbalance situation appears. Therefore, the record that used to analyze the unbalance components is from the substation connecting two utilities.



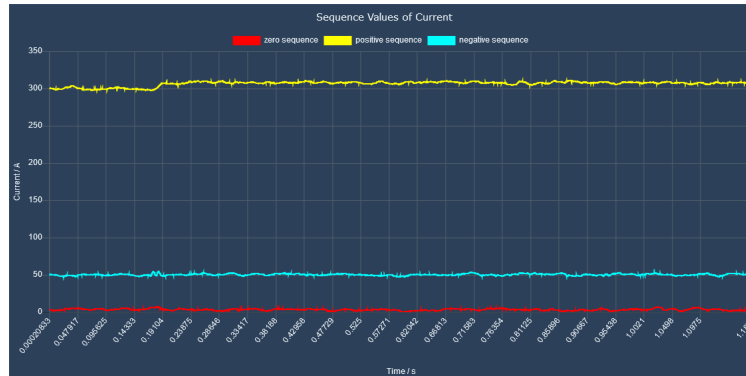
(a) Phasor estimation for current



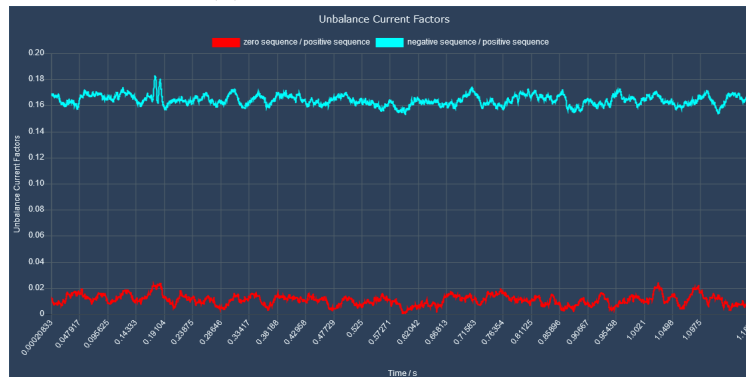
(b) IoVs of current

Figure 4.12: Phasor estimation for the substation connecting two utilities.

It's difficult to get unbalanced condition information from the phasor estimation. As shown in figure 4.12, the collected values and computed values are almost overlapping, and errors are small. However, it can be implied from figure 4.13 that there is a current unbalance issue.



(a) Current sequence values



(b) Unbalance factors

Figure 4.13: Unbalance components report for substation that connecting two utilities.

As presented in figure 4.13a, the positive sequence values are around RMS value of the phase current, and zero sequence values are near 0 amp. But the negative sequence values are stabilized at approximately 50 amps, which corresponds to 0.17 of the unbalance factor in figure 4.13b.

Since the imbalance systems can cause motor damage from excessive heat, increasing losses and unnecessary trip, it's needful to monitor the sequence values and unbalance factors.

With these reports, the damage can be significantly reduced and the incorrect operations can be eliminated.

4.2.4 Results With Fault And Their Analysis With Unbalanced Conditions

When a fault occurs in the substation or between the lines, the DFRs nearby will be triggered and the reports will be generated. However, it is difficult to indicate what type and reason of the fault. The unbalance analysis not only helps engineers to identify imbalance issues, but can also help fault analysis group troubleshoot the possible causes of an event.

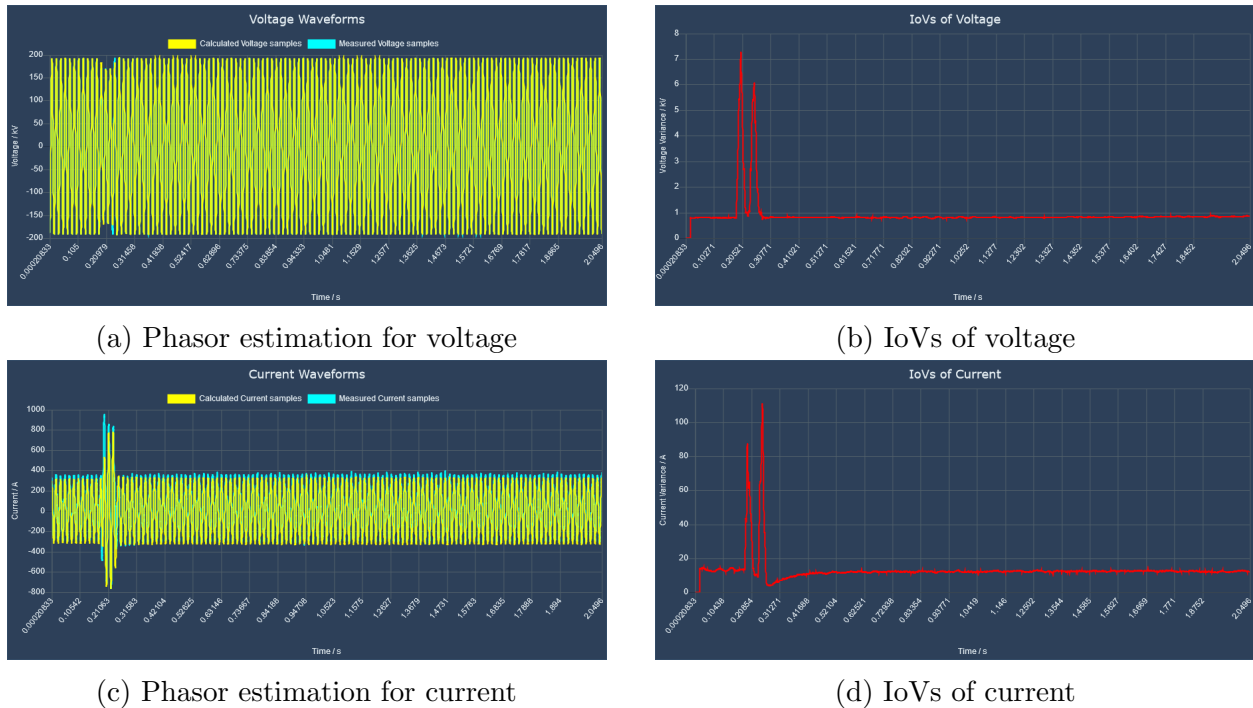
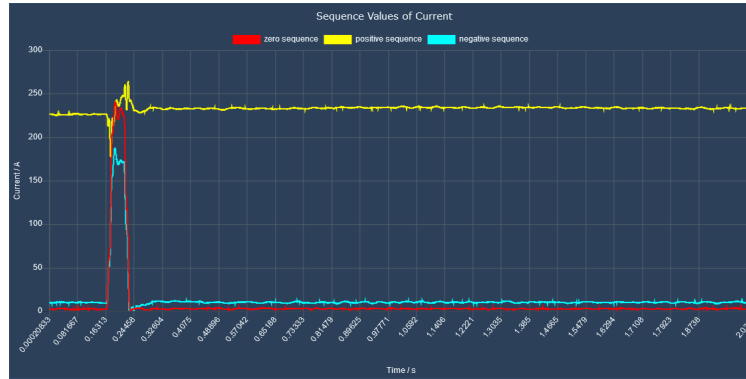


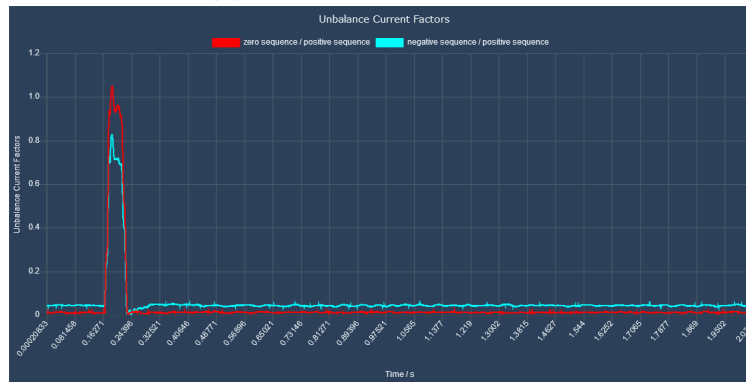
Figure 4.14: The first example results when an event occurs.

Figure 4.14 is an example of a fault event. The charts show that there is a fault around 0.19 second and it sustains about 0.06 second. The voltage drops during the event while

the current is rising. Combined with the unbalance components as shown in figure 4.15, one possible reason can be concluded.



(a) Current sequence values



(b) Current unbalance factors

Figure 4.15: The first example reports of current unbalance components when an event occurs.

From the figure 4.15a, it can be observed that the zero sequence and negative sequence values are almost as same as positive values during the fault. This can also be proved by figure 4.15b, both ratios are above 0.8. Therefore, $I_0 \approx I_1 \approx I_2$. As a consequence, the fault can be a phase-to-ground fault. There is also an another possible reason for this fault. If the substation is connected to a wye-delta transformer, a phase-to-ground fault will become a phase-to-phase-to-ground fault. As a result, the original fault might be phase-to-ground fault or double-phase-to-ground fault.

The second sample example is shown in figure 4.16. The event started at 0.188 second

and ended at 0.237 second, and voltage drops while current rising during the fault. To figure out the possible reasons, the unbalanced condition needs to be analyzed.

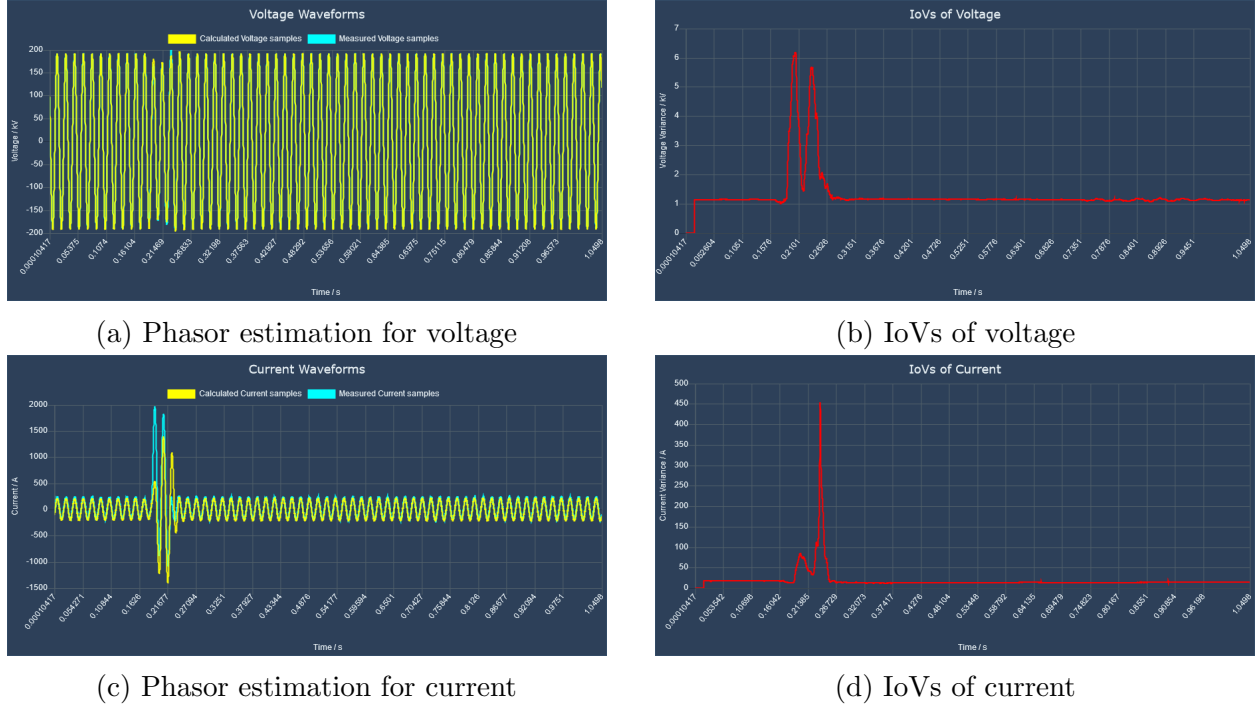
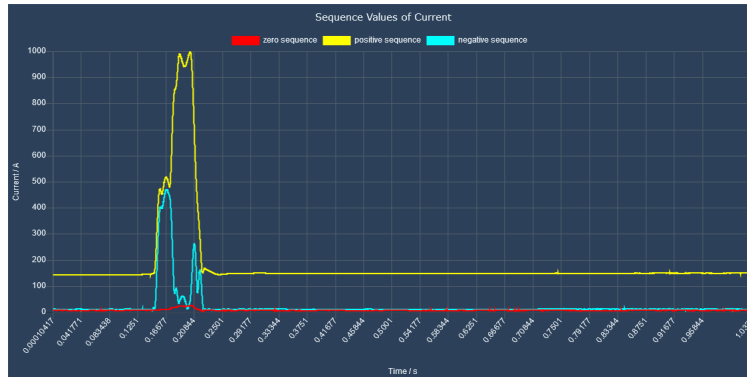


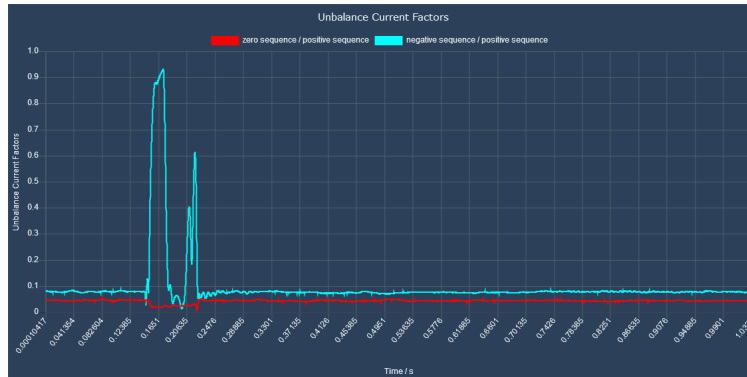
Figure 4.16: The second example results when a fault occurs.

Figure 4.17 presents the unbalance analysis for second example. In the beginning, from 0.15 to 0.17 second, the negative sequence values are almost equal to positive values, and the zero sequence values maintain at 0 amp. It can be also proved from figure 4.17b since the unbalance factors based on negative values are about 1 during that time. It can be a phase-to-phase fault as $I_1 \approx I_2$, and $I_0 = 0$.

From 0.17 second to 0.22 second, the negative sequence current drops to zero and positive sequence values go up. For this situation: $I_1 \approx I_a$, $I_0 \approx I_2 \approx 0$. As a result, the fault seems become a three-phase fault in the end.



(a) Current sequence values



(b) Current unbalance factors

Figure 4.17: The second example reports of current unbalance components when an event occurs.

Those two examples are all from the substations that sensed the fault but didn't trip since the faults didn't belong to them. The event occurred somewhere else and the fluctuations were spread out. These records are important since the impact of a fault through distance can be analyzed in the future. And it might be possible to locate a fault based on this research result.

Chapter 5

Conclusion and Future Work

5.1 Summary

The main goal of this project is to analyze the power quality and unbalanced conditions by using the records from digital fault recorders. In this project, voltage and current variation, harmonic contents and unbalance components are completed and presented in a web dashboard.

The first step is to obtain the data from DFRs based on COMTRADE standard. The information of the data such as sampling rate, initial time, line frequency can be decoded from a configuration file, and collected samples can be read out through a data file. After the data has been acquired, a program will be launched to accomplish all the analyses.

Phasor estimation is the essential step for the rest analyses. Recursive algorithm is applied to calculate the phasor for each point in time, and the IoVs are also computed. If the IoV is beyond the threshold value, the harmonic contents analysis will be triggered. Fast Fourier Transform is the method that is utilized in this thesis. To avoid aliasing problem,

the bandwidth for the spectrum is limited within half of the sampling rate. Since the power is from infinite systems, the voltage is stable and barely influenced by an event. Thus, the project just analyzed the current harmonics and current unbalance components. For unbalance analysis, symmetric components need to be calculated from three-phase value firstly. The ratio of negative sequence value and positive sequence value as well as the ratio of zero sequence value and positive sequence value are computed as unbalance factors in this paper. Under normal condition, both ratios should be around zero.

When all the computation completed, the collected data and the outputs from calculation will be stored in a database. And the last step is to develop the web dashboard for those reports. JavaScript, HTML5 and some web tools are applied to accomplish the web page. The start page is the google map with all the DFR markers, and it will switch to a report page after double-clicking the marker.

The details and interpretations for each case of the report are also included in this thesis. Besides the explanation for the normal case, harmonic contents and unbalance components and the study of fault assessment based on unbalanced conditions are also presented.

With the dashboard developed in this paper, engineers can monitor the historical data from DFRs. At the same time, they can also check the harmonic contents and unbalance components to gather information to analyze power quality problems. What's more, the protection group can combine the unbalanced conditions to identify the possible causes and characteristics of a fault.

5.2 Future Work

This thesis is just an initialization of a power quality dashboard and there are wide range of works that can be achieved through it. First of all, a warning feature can be accomplished. When the harmonic contents or the sequence values are under abnormal status, the color of the marker in the map can be changed as a sign of warning. Another thing that can be achieved is the harmonic gradient mapping. The impact of harmonics can be gradually reduced from the central point to the surrounding. In the future, after all the DFRs can communicate with each other based on IEC61850 standard, the DFRs nearby will also be triggered when there is an event occurring at the central DFR. Therefore, the harmonic reports will be generated for all of them and can be presented as gradient colors in the map.

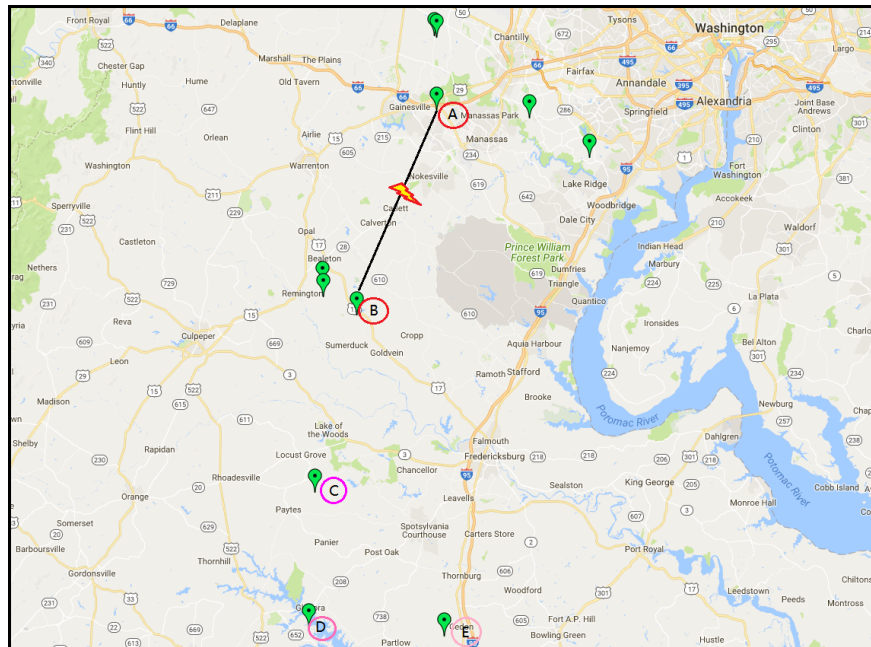


Figure 5.1: The analysis of the impact of a fault through the distance

Besides, the impact of a fault through the distance can be achieved by utilizing the analytical result from symmetrical components. For example, from figure 5.1, a fault oc-

curred between A and B. Records and analysis results from B, C, D and E can be utilized to compare the computed values, IoVs and symmetrical components.

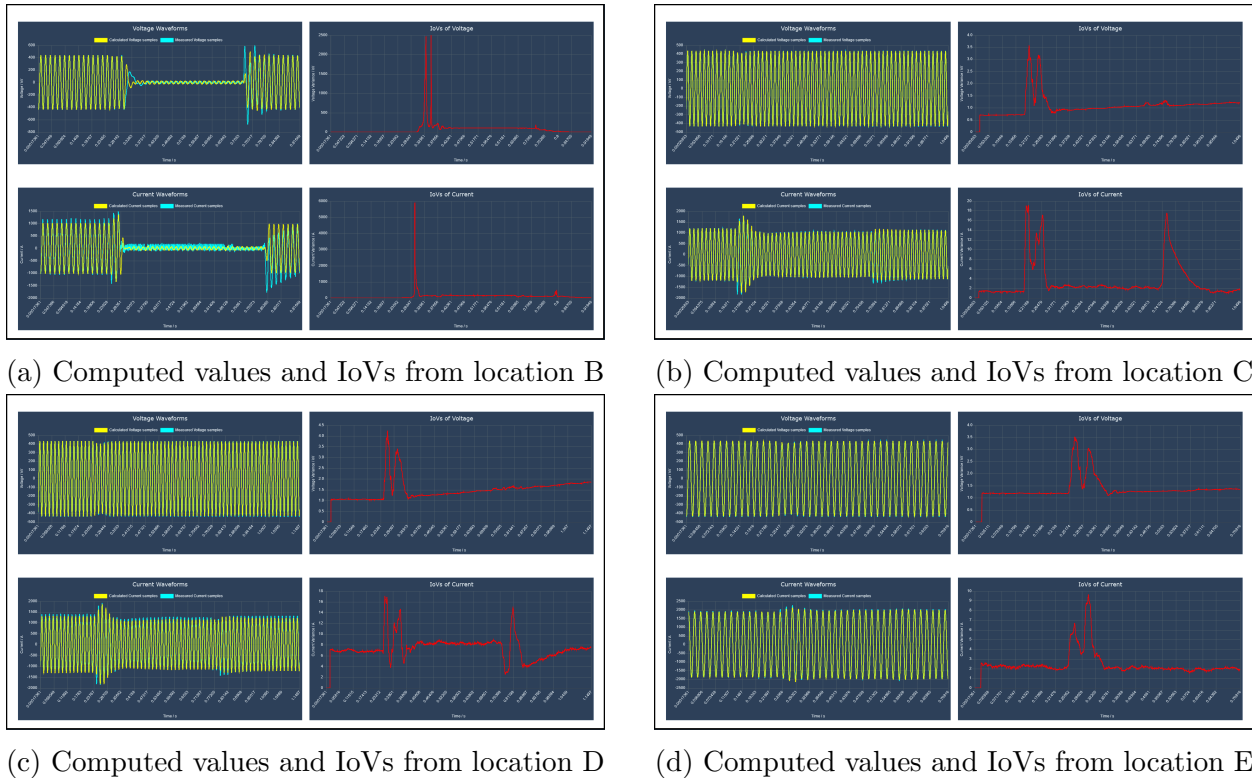
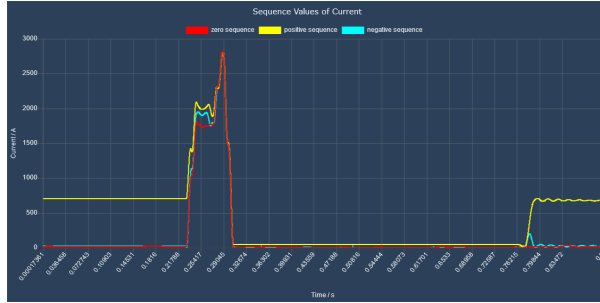
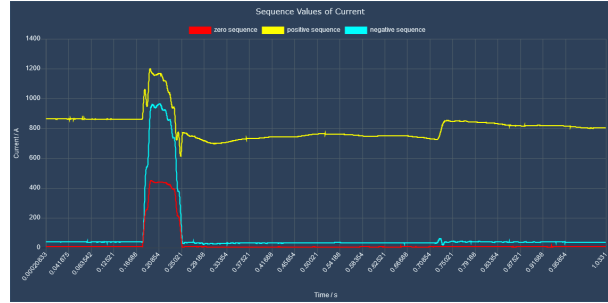


Figure 5.2: Comparison of computed values and IoVs from locations B, C, D, E

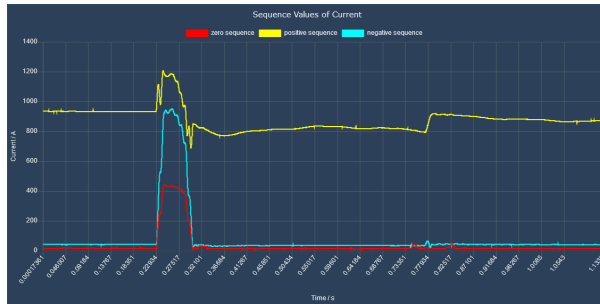
Figure 5.2 presents the comparison of computed sample values and IoVs. Before the circuit breaker (CB) trip, the voltage from substation B dropped and current went up. Both the voltage and current dropped to zero when CB is opened, and they were back to steady status after CB is re-closed. The IoV of current was as high as 6000 amps during the fault. Since substation C, D and E were not responsible for the event, they were still influenced by the fault and generated the records. Voltage and current variations can be seen from figures 5.2b, 5.2c and 5.2d. And with the increase of the distance from location B, the fluctuation of voltage and current was decreased. The current IoV during the fault in substation E was just 6.5 amps.



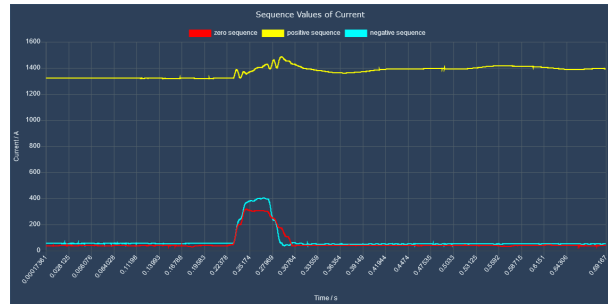
(a) Symmetrical components from location B



(b) Symmetrical components from location C



(c) Symmetrical components from location D



(d) Symmetrical components from location E

Figure 5.3: Comparison of symmetrical components from locations B, C, D, E

The comparison of symmetrical components from those four substations is shown in figure 5.3. In substation B, during the event, positive sequence values, negative sequence values and zero sequence values were almost equal to each other, which indicate a phase-to-phase fault. However, from locations C, D and E, those three sequence values were no longer equal during the fault. It may indicate a double-phase-fault from substation C or D since $I_2 + I_0 = I_1$. Or it can be a phase-to-phase fault on the other side if the substation is connected to a wye-delta transformer. And it is difficult to indicate the possible reason from location E.

Therefore, it might reach a conclusion that the impact of a fault is decreasing while the distance from the fault location is larger. And by analyzing large quantity of records, it is possible to estimate the distance between the fault location and the substation the records the event.

Reference

- [1] R. C. Dugan, M. F. McGranaghan, S. Santoso, and H. W. Beaty, *Electrical Power Systems Quality*. New York, NY: McGraw-Hill Education, 2 ed., 2002.
- [2] R. C. Sermon, “An overview of power quality standards and guidelines from the end-user’s point-of-view,” in *Rural Electric Power Conference 2005*, (San Antonio, TX), IEEE, May 2005.
- [3] P. Pillay and M. Manyage, “Definition of voltage unbalance,” *IEEE Power Engineering Review*, vol. 21, pp. 49–51, May 2001.
- [4] J. Perez and C. Rincon, “A guide to digital fault recording event analysis,” in *2010 63rd Annual Conference for Protective Relay Engineers*, (College Station, TX), IEEE, May 2010.
- [5] J. Wang, X. Li, and S. Su, “Research on the application of the recorded fault data analysis based on comtrade standard in electric power load modeling,” in *Power Engineering Conference, 2005. IPEC 2005. The 7th International*, (Singapore, Singapore), IEEE, 08 May 2006.
- [6] P. S. R. C. of The IEEE Power Engineering Society, “Ieee standard common format for transient data exchange (comtrade) for power systems,” 1999.
- [7] M. Z. Alias and M. S. Shokri, “The design of iec 61850 based disturbance and fault recorder for online fault analysis in system verification and simulation laboratory,” in *2015 International Symposium on Technology Management and Emerging Technologies (ISTMET)*, (Langkawai Island, Malaysia), IEEE, 17 December 2015.
- [8] “Every day big data statistics - 2.5 quintillion bytes of data created daily.” <http://www.vcloudnews.com/every-day-big-data-statistics-2-5-quintillion-bytes-of-data-created-daily/>, 2015.
- [9] Y. Guo, S. Feng, and K. Li, “Big data processing and analysis platform for condition monitoring of electric power system,” in *2016 UKACC 11th International Conference on Control (CONTROL)*, (Belfast, UK), IEEE, November 2016.

-
- [10] H. Huang and X. Zou, "Implementation of model-driven visualizations in dominion energy," in *2017 Grid of the Future Symposium*, (Cleveland, Ohio), CIGRE US National Committee, October 2017.
- [11] M. G. Krishnan and S. Ashok, "Implementation of recursive dft algorithm for phasor measurement unit (pmu)," in *2012 IEEE International Conference on Engineering Education: Innovative Practices and Future Trends (AICERA)*, (Kottayam, India), IEEE, July 2012.
- [12] Z. Gao, H. Zhao, and X. Zhou, "Summary of power system harmonics," in *2017 29th Chinese Control And Decision Conference (CCDC)*, (Chongqing, China), IEEE, July 2017.
- [13] B. A. Olshausen, "Aliasing psc 129 - sensory processes." <http://redwood.berkeley.edu/bruno/npb261/aliasing.pdf>, 2000.
- [14] "Current and voltage unbalance- causes and counter measures." <https://zenatix.com/current-and-voltage-unbalance-causes-and-counter-measures/>, 2015.
- [15] "6 phases of the web site design and development process." <https://www.idesignstudios.com/blog/web-design/phases-web-design-development-process/#.Wgsi6WhSyUk>.
- [16] N. Phannil, C. Jettanasen, and A. Ngaopitakkul, "Power quality analysis of grid connected solar power inverter," in *2017 IEEE 3rd International Future Energy Electronics Conference and ECCE Asia (IFEEC 2017 - ECCE Asia)*, (Kaohsiung, Taiwan), IEEE, June 2017.
- [17] P. Bornard, J. M. Tesserson, J. C. Bastide, and M. Nourris, "Field experience of digital fault recorders and distance relay in ehv substations," *IEEE Power Engineering Review*, vol. PER-4, pp. 38–38, January 1984.
- [18] C. Mikkelsen, J. Johansson, and M. Cooper, "Visualization of power system data on situation overview displays," in *2012 16th International Conference on Information Visualisation*, (Montpellier, France), IEEE, September 2012.
- [19] D. Yang, "A power system network partition framework for data-driven regional voltage control," in *2017 North American Power Symposium (NAPS)*, (Morgantown, WV), IEEE, September 2017.